Acta Cryst. (1983). B39, 239–243

The Charge Density Distribution in $LiAlB_{14}$

BY TETSUZO ITO AND IWAMI HIGASHI

The Institute of Physical and Chemical Research, Wako-shi, Saitama 351, *Japan*

(*Received* 20 *October* 1982; *accepted* 7 *December* 1982)

Abstract

The charge density distribution in $LiAlB_{14}$ has been investigated by X-ray diffractometry. Population analysis of valence electrons with a least-squares method ($R = 0.019$, $R_w = 0.035$ for 1895 reflections) resulted in a net charge distribution of Li^{1+}-$(Al^{1.7+})_{0.96}(B_{12})^{1.2-}.2B^{0.7-}$. On the other hand, charge integration around the metal atoms within the spheres of radii 1·08 and 1·15 Å for Li and Al respectively gave net charges of $Li^{0.7+}$ and $Al^{1.5+}$. These results indicate that the structure of $LiAlB_{14}$ is stabilized by charge transfer from the metals to the electron-deficient boron framework. Deformation maps through the triangular faces of the B_{12} icosahedron showed accumulation of charges at the centers of the faces, which is a characteristic feature of delocalized three-center bonds. The bonding-electron peaks of the strained intericosahedral B–B bonds are not located on the bonds but shifted toward the pseudo fivefold axes of the icosahedron, indicating that the bonds are bent. Around the metal atoms prominent peaks were observed which are much sharper and closer to the atomic centers than expected for the valence electrons of free metal atoms.

Introduction

Boron icosahedra and fused icosahedra are basic structural units in elementary borons and metal higher borides (Naslain, 1977). A previous X-ray study on α-AlB_{12} (Ito, Higashi & Sakurai, 1979) has shown that the bonds within the icosahedral units are highly delocalized bonds, whereas the intericosahedral B–B bonds are localized two-center bonds. On the other hand, Higashi (1980) has investigated charge balance among different boron units in several α-AlB_{12}-type compounds by counting the number of contacts between the metal atoms and boron units. In the present work, the charge density distribution in $LiAlB_{14}$ has been investigated in order to elucidate the role of the metal atoms in stabilizing the structure.

Experimental

The crystal structure of $LiAlB_{14}$ has already been reported (Higashi, 1981). The crystal is orthorhombic

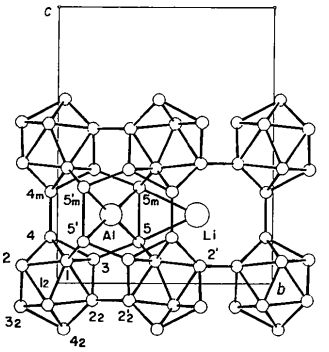

Fig. 1. Projection of the structure along the *a* axis ($0 \le x \le \frac{1}{4}$).

with $a = 5.847$ (1), $b = 8.143$ (1), $c = 10.354$ (1) Å, $Z = 4$ and space group *Imam*. As shown in Fig. 1, the structure consists of a network of B_{12} icosahedra [B(1), B(2), B(3) and B(4)] and single boron atoms [B(5)] with interstitial Li and Al atoms.

A plate-like crystal with dimensions 0·53 × 0·52 × 0·14 mm was selected for the present study. Intensity data were collected on a Rigaku automated four-circle diffractometer using graphite-monochromated Mo $K\alpha$ radiation. The crystal was rotated in an ω-scan mode up to $2\theta = 30°$ and ω–2θ mode up to $2\theta = 120°$ ($\sin\theta/\lambda = 1.22$ Å^{-1}) at a rate of 2° min^{-1} in ω. Background counts of 10 s were measured on each side of the scan width of $\Delta\omega = (1.2 + 0.5 \tan\theta)°$. Three standard reflections were monitored after every 100 reflections and variations of the F_o's were less than 0·5%. A total of 3472 reflections (hkl and $\bar{h}k\bar{l}$) with $F_o > 3\sigma_{count}(F_o)$ were obtained, where $\sigma_{count}(F_o)$ is the standard deviation estimated from the counting statistics. After Lorentz, polarization and absorption [μ(Mo $K\alpha$) = 2·483 cm^{-1}] corrections, equivalent reflections were averaged to give 1895 unique reflections. The internal consistency factor $R_{int}[= \sum\sigma_{diff}(F_o)/\sum F_o]$ was 0·012, where $\sigma_{diff}(F_o)$ is the standard deviation estimated from the discrepancies of F_o's among equivalent reflections.

Results and discussion

Neutral-atom refinement

Structure refinement started from the results of the previous paper (Higashi, 1981) assuming at first that all

0567-7408/83/020239-05$01.50

Table 1. *Atomic coordinates with e.s.d.'s in parentheses* ($\times 10^5$) *from the HO refinement*

The occupancy factor of Al is 0·9594 (25).

	x	*y*	*z*
Li	0	35141 (20)	75000
Al	25000	25000	25000
B(1)	25002 (2)	4366 (1)	7982 (1)
B(2)	15942 (2)	83560 (1)	6237 (1)
B(3)	0	16997 (2)	8524 (2)
B(4)	0	−3184 (2)	16680 (2)
B(5)	0	37948 (2)	14959 (2)

Table 2. *Scale and agreement factors of the least-squares refinements*

$R = \sum |F_o - F_c| / \sum F_o$, $R_w = [\sum w(F_o - F_c)^2 / \sum wF_o^2]^{1/2}$ and S (goodness of fit) $= [\sum w(F_o - F_c)^2/(m-n)]^{1/2}$.

Refinement	HO	ALL	ELS
$\sin\theta/\lambda$ (Å^{-1})	0·7–1·22	0·0–1·22	0·0–1·22
No. of reflections, *m*	1493	1895	1895
No. of variables, *n*	47	32	38
Scale factor	0·977 (1)	1·000 (2)	1·000 (1)
R	0·015	0·020	0·019
R_w	0·014	0·043	0·035
S	1·3	5·3	4·4

the atoms are neutral. The full-matrix least-squares program *RADIEL* (Coppens, Guru Row, Leung, Stevens, Becker & Yang, 1979) was used. The atomic scattering factors and the dispersion correction factors were taken from *International Tables for X-ray Crystallography* (1974).

In order to reduce bias due to bonding effects, refinement was first performed using 1493 high-order (HO) data with $\sin\theta/\lambda > 0{\cdot}7$ Å^{-1}. The function minimized was $\sum w|F_o - F_c|^2$. The weight was chosen as $w = \sigma^{-2}$, where σ was the larger of the two standard deviations, $\sigma_{count}(F_o)$ and $\sigma_{diff}(F_o)$. The occupancy factors of Li and Al were also varied in this refinement; they turned out to be 1·00 (3) and 0·959 (3) for Li and Al, respectively. The atomic coordinates are given in Table 1; they are in agreement with those reported previously (Higashi, 1981) within the estimated standard deviations.

In the HO refinement, significant correlations were noted between the scale factor and the anisotropic temperature factors. In fact, by changing the lower cut-off point of $\sin\theta/\lambda$ from 0·8 (1304 reflections) to 0·6 Å^{-1} (1635 reflections), the scale factor k (defined as $F_o = kF_c$) increased by 1·4% and the equivalent isotropic temperature factors systematically increased by about 4%. Moreover, on the deformation maps calculated with the scale factor of the HO refinement, sharp peaks of about 0·3 e Å^{-3} appeared at all the atomic positions. In the next step, therefore, the scale factor and the temperature factors were refined using all the 1895 reflections (ALL); the atomic coordinates and the occupancy factors were fixed at the HO values. The scale factor increased by 2·3% from that of the HO refinement. The scale and agreement factors of various least-squares refinements are compared in Table 2.

Population refinement

The extended *L*-shell (ELS) refinement (Coppens, Pautler & Griffin, 1971) was next performed; the populations, *p*, of valence electrons of the individual atoms were varied together with the scale factor and the anisotropic temperature factors. The total charge was kept constant by imposing a neutrality constraint. The core- and the valence-electron scattering factors were taken from *International Tables for X-ray Crystallography* (1974). The valence-electron scattering factor for the Li atom was assumed as the difference between the scattering factors for the neutral Li atom and the Li^{1+} ion. However, least-squares refinement resulted in a negative number of valence electrons for the Li atom [p(Li) = −1·1 (3)]; this was probably because the scattering factor used was inappropriate to represent the real valence-electron distribution of the Li atom. In subsequent refinements, therefore, p(Li) was assumed to be zero (*i.e.* Li^{1+} was assumed). Although the isotropic extinction parameter, g, was varied in this refinement, extinction effects were not detected for this crystal; since g turned out to be slightly negative [$-0{\cdot}12\ (3) \times 10^{-4}$], it was assumed to be zero. By the ELS refinement, the scale factor remained unchanged from that of the ALL refinement (*cf.* Table 2). The anisotropic temperature factors obtained are given in Table 3.*

The populations of valence electrons are given in Table 4 in the form of net charges. As is evident from the table, substantial amounts of the valence electrons of Li and Al are transferred to B atoms. In particular, the B(5) and B(2) atoms which are in closer and more frequent contacts with the metal atoms (*cf.* Fig. 1 and Higashi, 1981) are most negatively charged. If the individual net charges of atoms B(1) to B(4) are

* A list of structure factors has been deposited with the British Library Lending Division as Supplementary Publication No. SUP 38272 (14 pp.). Copies may be obtained through The Executive Secretary, International Union of Crystallography, 5 Abbey Square, Chester CH1 2HU, England.

Table 3. *Anisotropic temperature factors with e.s.d.'s in parentheses* ($\times 10^5$) *from the ELS refinement*

The temperature-factor expression is $\exp(-2\pi^2 \sum_i \sum_j h_i h_j a_i^* a_j^* U_{ij})$.

	U_{11}	U_{22}	U_{33}	U_{12}	U_{13}	U_{23}
Li	5347 (138)	1456 (73)	1784 (79)	0	0	0
Al	650 (8)	1209 (9)	414 (6)	537 (6)	0	0
B(1)	431 (8)	427 (8)	419 (8)	0 (7)	−14 (7)	−15 (6)
B(2)	458 (8)	403 (8)	420 (7)	39 (7)	−7 (7)	−6 (6)
B(3)	439 (12)	427 (12)	411 (11)	0	0	−32 (9)
B(4)	458 (12)	454 (12)	353 (11)	0	0	−8 (9)
B(5)	391 (12)	443 (12)	484 (11)	0	0	39 (9)

Table 4. *Net charges with e.s.d.'s in parentheses from the ELS refinement*

Li	1·00+	B(3)	0·06 (3)–
Al	1·69 (8)+	B(4)	0·09 (2)+
B(1)	0·04 (1)–	B(5)	0·71 (3)–
B(2)	0·27 (2)–		

summed, the net charge distribution among the chemical units of the crystal can be expressed as $Li^{1+}(Al^{1\cdot7+})_{0\cdot96}(B_{12})^{1\cdot2-}.2B^{0\cdot7-}$.

Charge integration

The net charges of the Li and Al atoms were estimated also by integrating the charge densities within a sphere of radius R around each metal-atom position using the computer program *CHAR* (Kobayashi, Marumo & Saito, 1972). The observed radial distribution curves $D(R)$ for the Li and Al atoms are shown in Fig. 2. Each $D(R)$ curve is characterized by a main peak followed by a subsidiary hump at R of about 1·0 Å. These humps come from the electron densities in intermediate regions between the metal and surrounding boron atoms as can be seen from the shortest metal–boron distances of 2·42 and 2·08 Å for the Li and Al atoms, respectively. Therefore, in the present analysis an effective atomic radius, R_{eff}, of each metal atom was defined as the radius corresponding to the maximum of the hump. The R_{eff} values for the Li and Al atoms are 1·08 and 1·15 Å respectively, and the corresponding net charges are $Li^{0\cdot7+}$ and $Al^{1\cdot5+}$, which are in fairly good agreement with the net charges Li^{1+} and $Al^{1\cdot7+}$ estimated by the population refinement.

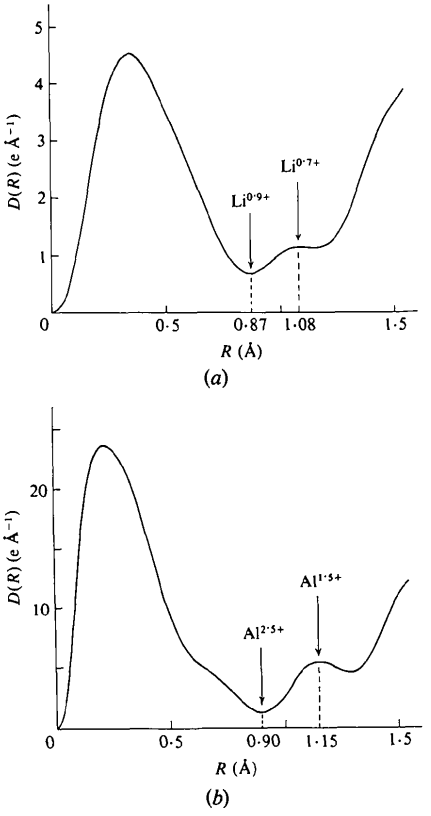

Fig. 2. Radial distribution curves of the total electrons around (*a*) Li and (*b*) Al atoms.

It should be noted that there remains necessarily some arbitrariness in the definition of an electron population or a net charge of an atom because they are only working parameters. However, from the close agreement between the two sets of net charges, it may be concluded that more than a half of the valence electrons of the metal atoms are transferred to the electron-deficient boron framework to stabilize the structure.

Deformation densities

Deformation densities through various sections of the structure were calculated using the scale and phase factors obtained by the neutral-atom refinement. The high-order reflections with $\sin\theta/\lambda > 1\cdot0$ Å^{-1} were excluded from the calculation to reduce noise peaks irrelevant to the deformations of valence electrons. Distributions of the residual peaks around the B_{12} icosahedron were similar to those in α-AlB_{12} (Ito *et al.*, 1979). A broad peak of about 0·15 e Å^{-3}, characteristic of a delocalized three-center bond, is observed at the center of each triangular face of the icosahedron; an example is shown in Fig. 3.

Another interesting feature of the deformation densities can be seen in Fig. 4, a section through two opposite edges, B(3)–B(2_2) and B(2_m)–B(3_2), of the B_{12} icosahedron (a bisecting plane). The four external B–B bonds also lie approximately on the plane. The

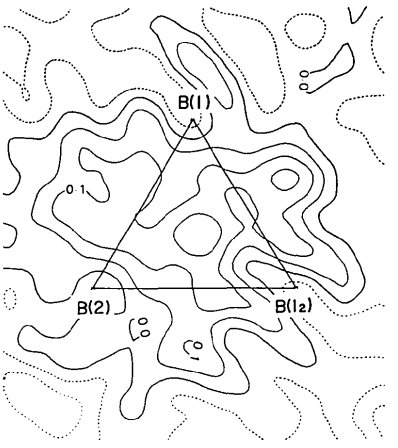

Fig. 3. Deformation densities through a triangular face of the B_{12} icosahedron. Contours at 0·05 e Å^{-3}; negative contours broken; zero contours thick.

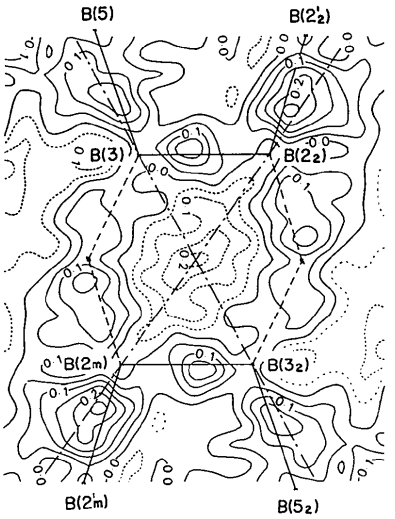

Fig. 4. Deformation densities through a bisecting plane of the icosahedron. Contours as in Fig. 3. The chain lines indicate pseudo fivefold axes.

prominent peaks of about 0·2 e $Å^{-3}$ around the external bonds indicate that these bonds are two-center bonds as were also noted in α-AlB_{12}. However, they do not lie on the B–B internuclear lines but are shifted toward pseudo fivefold axes (the chain lines) of the icosahedron along which apical boron atoms tend to form directional bonds. In other words, these external bonds are bent because the geometries of the bonds are highly strained; the angles between the internuclear lines and the pseudo fivefold axes are 22 and 11° for the B(2)–B(2′) and B(3)–B(5) bonds, respectively.

Deformation densities around the Li and Al atoms are shown in Figs. 5 and 6, respectively. Although there are diffuse peaks in intermediate regions between the metal and coordinating boron atoms, no localized peaks are observed on the metal–boron internuclear lines, which shows that metal–boron interactions are mainly ionic. On the other hand, the metal sites are surrounded by sharp peaks of about 0·2 e $Å^{-3}$; for the

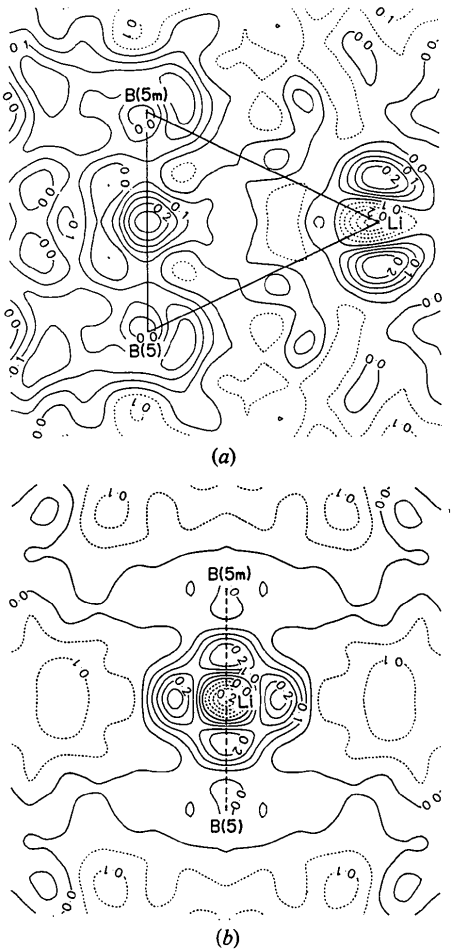

Fig. 5. Deformation densities around the Li atom: (*a*) the B(5)–Li–B(5) plane and (*b*) the plane through the Li atom, perpendicular to (*a*) and parallel to the B(5)–B(5) bond. Contours as in Fig. 3.

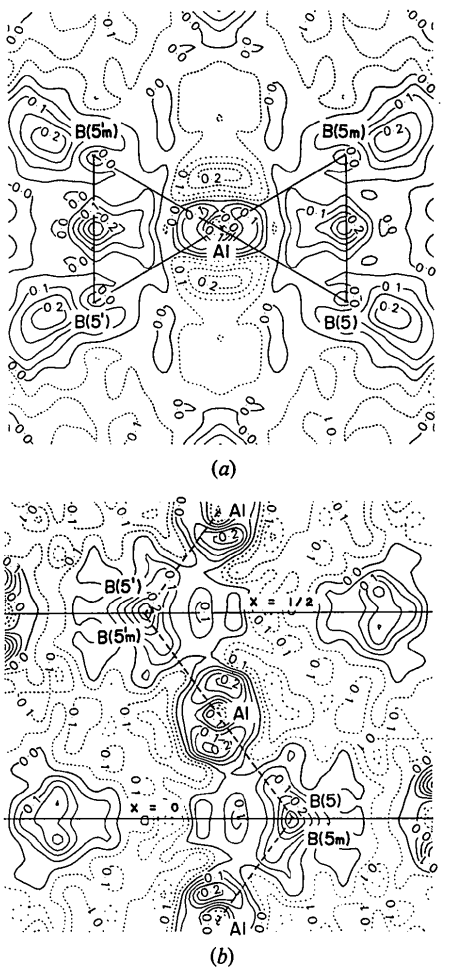

Fig. 6. Deformation densities around the Al atom: (*a*) the 4B(5) rectangular plane through the Al atom and (*b*) the (001) plane through the Al atom. Contours as in Fig. 3.

Li site (site symmetry *mm*), two pairs of peaks at 0·4 and 0·5 Å from the atomic center are arranged like a doughnut perpendicular to the B(5)—Li—B(5) plane and parallel to the B(5)—B(5) bond, whereas for the Al site (site symmetry 2/*m*), a pair of peaks at 0·5 Å from the atomic center are arranged like a sandwich approximately along the *a* axis. These peaks are much sharper and closer to the atomic centers than expected for the valence electrons of free metal atoms (2*s* electrons for Li and 3*s*, 3*p* electrons for Al). Further studies on related compounds will clarify whether these peaks represent real deformations of valence electrons or some other characteristics of the metal sites such as positional disorder. It is interesting to note that the shortest Al—Al distance (2·92 Å) is comparable to that (2·86 Å) in metallic aluminum, and the shortest Li—Li distance (3·36 Å) is a little longer than that (3·03 Å) in metallic lithium.

Calculations were performed on a FACOM M200 computer of this Institute using the *UNICS* III program system (Sakurai & Kobayashi, 1979) unless otherwise stated. We are grateful to Professor Y. Saito and Dr S. Ohba of Keio University for allowing us to use the computer programs *CHAR* and *RADIEL*. Our thanks are also due to Professor W. N. Lipscomb of Harvard University for his encouragement; in fact, he has correctly predicted a large amount of charge transfer from the metal to B(5) atoms, and also the bends in the highly strained B—B bonds.

References

COPPENS, P., GURU ROW, T. N., LEUNG, P., STEVENS, E. D., BECKER, P. J. & YANG, Y. W. (1979). *Acta Cryst.* A**35**, 63–72.

COPPENS, P., PAUTLER, D. & GRIFFIN, J. F. (1971). *J. Am. Chem. Soc.* **93**, 1051–1058.

HIGASHI, I. (1980). *J. Solid State Chem.* **32**, 201–212.

HIGASHI, I. (1981). *J. Less-Common Met.* **82**, 317–323.

International Tables for X-ray Crystallography (1974). Vol. IV. Birmingham: Kynoch Press.

ITO, T., HIGASHI, I. & SAKURAI, T. (1979). *J. Solid State Chem.* **28**, 171–184.

KOBAYASHI, A., MARUMO, F. & SAITO, Y. (1972). *Acta Cryst.* B**28**, 2709–2715.

NASLAIN, R. (1977). *Boron and Refractory Bromides*, edited by V. I. MATKOVICH pp. 139–202. Berlin: Springer-Verlag.

SAKURAI, T. & KOBAYASHI, K. (1979). *Rep. Inst. Phys. Chem. Res.* **55**, 69–77.

Acta Cryst. (1983). B**39**, 243–250

Crystalline-State Reaction of Cobaloxime Complexes by X-ray Exposure. V. A New Type of Racemization Caused by the Cooperative Motion of Two Reactive Groups

BY TOSHIHARU KURIHARA, YUJI OHASHI* AND YOSHIO SASADA

Laboratory of Chemistry for Natural Products, Tokyo Institute of Technology, Nagatsuta, Midori-ku, Yokohama 227, Japan

AND YOSHIAKI OHGO

Niigata College of Pharmacy, 5829 Kamishinei-cho, Niigata 950–21, Japan

(*Received* 18 *September* 1982; *accepted* 1 *November* 1982)

Abstract

Crystalline-state racemization has been found at 353 K for a crystal of (4-chloropyridine)bis(dimethylglyoximato)[(*R*)-1-methoxycarbonylethyl]cobalt(III) (dimethylglyoximato = 2,3-butanedione dioximato), $C_{17}H_{25}ClCoN_5O_6$, $[Co(C_5H_4ClN)(C_4H_7N_2O_2)_2(C_4H_7O_2)]$. When the temperature is lowered to 293 K, the racemization is no longer observed. The crystal at the initial stage at 293 K is monoclinic, space group $P2_1$, with a = 14·946 (2), b = 9·227 (1), c = 15·956 (3) Å, β = 103·95 (2)°, V = 2135·5 (6) Å^3, M_r = 489·8, D_m = 1·52, D_x = 1·523 g cm^{-3} for Z = 4 and μ(Mo $K\alpha$) = 10·06 cm^{-1}. The unit-cell dimensions gradually vary with or without X-ray irradiation at 353 K and the space group changes to $P2_1/n$. The reaction follows approximate first-order kinetics. The rate constant is 6·88 × 10^{-5} s^{-1} at 353 K. The crystal structures at the initial and final stages at 293 K were solved by the direct method and refined by constrained least squares to R = 0·076 for 3383 reflections and R = 0·12 for 2572 reflections, respectively. The two crystallographically independent molecules at the initial stage are related by a pseudo inversion, which becomes

* To whom correspondence should be addressed.

0567-7408/83/020243-08$01.50